Spin Transport in High-Quality Suspended Graphene Devices

Guimaraes, Marcos H. D.; Veligura, A.; Zomer, P. J.; Maassen, T.; Vera-Marun, I. J.; Tombros, N.; van Arees, B. J.; Wees, B.J. van

Published in:
Nano Letters

DOI:
10.1021/nl301050a

Publication date:
2012

Spin transport in high quality suspended graphene devices

Marcos H. D. Guimarães,* A. Veligura, P. J. Zomer, T. Maassen, I. J. Vera-Marun, N. Tombros, and B. J. van Wees

Physics of Nanodevices, Zernike Institute for Advanced Materials, University of Groningen, The Netherlands

E-mail: m.h.diniz.guimaraes@rug.nl

Device Preparation

The devices are prepared in a similar fashion as the ones described by Tombros et al.,[1] although a few changes were made in order to avoid degradation of our high resistive contact barriers. First a 1 μm thick lift-off resist (LOR) film is spin-coated on a Si/SiO_2 (500 nm) substrate and the graphene flakes are exfoliated on top. Single layer flakes are then selected by optical contrast using a green filter.[2,3] For the electron beam lithography (EBL) process, to improve the undercut, we use a double layer Polymethyl methacrylate (PMMA) 50/410K resists dissolved in chlorobenzene and o-Xylene respectively. These solvents are used to prevent the removal of the LOR film during spin-coating. The contacts are then patterned and developed in n-Xylene (20^o C).

Using an electron beam evaporator with a base pressure lower than 8×10^{-7} Torr, we deposit 0.4 nm of Aluminium followed by *in-situ* oxidation by pure Oxygen gas at a pressure higher than 1×10^{-2} Torr for 15 minutes and the chamber is pumped down to the initial base pressure. This

*To whom correspondence should be addressed

process is performed twice in order to get contact resistances higher than 10 kΩ. After the high resistance barriers are deposited the chamber is pumped down to the initial base pressure and 60 nm of Cobalt is evaporated. For some of the studied samples in this work the electrodes were capped by 3 nm of Al_2O_3 to prevent Co oxidation. The lift-off is done in hot (75^o C) n-Xylene.

To suspend the graphene flakes a second EBL step is performed with an area dose of 510 μC/cm^2 and developed in 1-methyl 2-propanol. It was found that if the sample is immersed in Ethyl-lactat as described by Tombros et al.[1] the AlOx barriers degrade, causing a very large increase in the contact resistance and loss of the spin-signal. After this final process the sample is bonded and loaded in a cryostat which is pumped down to a base pressure lower than 1×10^{-6} Torr.

Current annealing

After the sample is loaded in the cryostat and characterized, we perform a current annealing step to remove the impurities in the graphene flake and obtain a high mobility device. The whole procedure is carried at 4.2 K.

To avoid degradation of the electrodes used for spin injection/detection, we apply the large DC bias for the current annealing in the two outer electrodes as depicted in Figure 1. The contact resistance of the inner contacts were measured before and after the current annealing step and showed no noticeable change.

We use a DC current bias-voltage compliance procedure to limit the power in our devices and avoid them to burn. The current is ramped up slowly (≈ 1 μA/s) until a determined value and then rapidly ramped down, at a rate 4 times faster than the ramping up. After each sweep in current we check the gate-voltage dependence on the sheet resistance to keep track of the device's mobility. For our samples, this current annealing procedure had a success rate of about 33% (4 out of 12 regions showed high mobility), comparable with our previous results.[1] One of the regions was current annealed twice. The first procedure resulted in a mobility of $\mu \approx 10^5$ cm^2/Vs, and after the

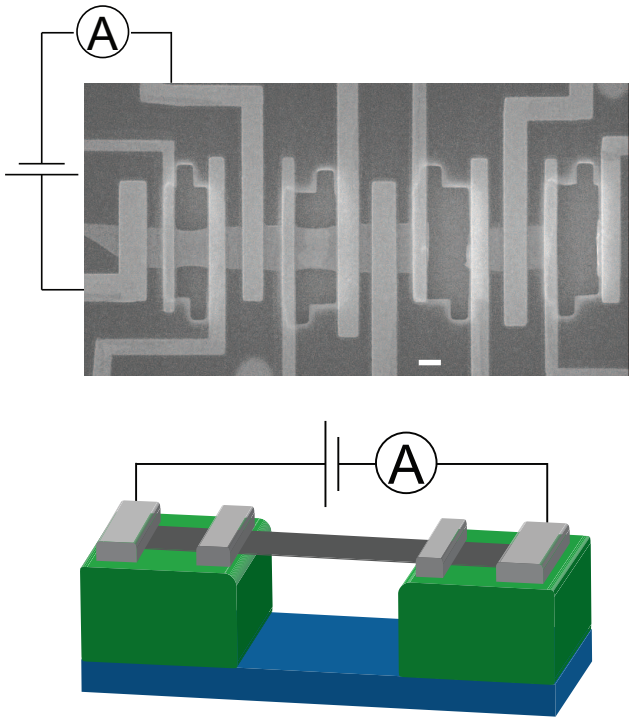

Figure 1: Top: A SEM picture of a typical device showing the schematics for the current annealing setup. On the left of the picture it can be seen two regions of suspended graphene flake, the outermost left successfully cleaned. On the right it can be seen two broken regions due to failing in the current annealing procedure. The scale bar measures 1 μm. Bottom: A cartoon illustrating the current annealing setup for comparison.

second current annealing the mobility was improved to $\mu \approx 3 \times 10^5$ cm^2/Vs. Despite performing spin-transport measurements in this sample, we also obtained spin signals in another sample with similar properties.

Details on the simulation

To represent our sample we extended the 1D model by Popinciuc et al.[4] to include three different regions: two semi-infinite outer parts of width W sandwiching one inner part of length L and width W. In this model we solve the stationary Bloch equations for the three components of the spin accumulation $\vec{\mu}_s(x)$ in the presence of a magnetic field $\vec{B}$:

$$D_s \nabla^2 \vec{\mu}_s - \frac{\vec{\mu}_s}{\tau_s} + \gamma \vec{B} \times \vec{\mu}_s = 0 \tag{1}$$

where D_s is the spin diffusion constant, τ_s is the spin relaxation time and $\gamma = g\mu_b \hbar^{-1}$ is the gyromagnetic ratio. All the parameters of the equation above can be set separately for each of the three regions, but for simplicity we make the two outer regions identical. For the boundary conditions we take:

1. $\mu_s(x = \pm\infty) = 0$
2. $\mu_s(x = 0_+) = \mu_s(x = 0_-)$
3. $\mu_s(x = L_+) = \mu_s(x = L_-)$
4. $\beta = \frac{\sigma_o W}{2e} \frac{d\mu_s(x=0_-)}{dx} - \frac{\sigma_i W}{2e} \frac{d\mu_s(x=0_+)}{dx} + \frac{\mu_s(x=0)}{2eR_{c1}}$
5. $0 = \frac{\sigma_i W}{2e} \frac{d\mu_s(x=L_-)}{dx} - \frac{\sigma_o W}{2e} \frac{d\mu_s(x=L_+)}{dx} + \frac{\mu_s(x=L)}{2eR_{c2}}$

where $\beta = \frac{PI}{2}$ for the x component of μ_s and $\beta = 0$ for the y and z components, with P being the spin polarization of the charge current I injected in the left boundary. The contact resistance of the contact at the left (right) boundary is represented by $R_{c1(c2)}$, and the conductivity of the inner (outer) regions by $\sigma_{i(o)}$. The contact induced spin relaxation is represented by the last term of items

4 and 5,[4] although contact effects were found to be negligible for our results when we consider values obtained experimentally in our samples.

We have to study the effect of four different parameters: the spin diffusion constants D_i and D_o, and the spin relaxation times τ_i and τ_o, where the subscripts "i" and "o" refer to the inner and outer regions respectively. In this analysis we kept the conductivities of the inner and outer regions fixed at: $\sigma_i = \sigma_o = 10^{-3}\Omega^{-1}$. In order to be able to observe the effect of each one of the parameters separately we calculated several Hanle precession curves keeping three of them constant and vary the remaining one. The simulated precession curves for a few sets of parameters are depicted in Figure 2. These curves were then fitted using the solution for the Bloch equations in a homogeneous system, like we fit our experimental results. From these fits we obtain an "effective" spin diffusion constant D_{fit} and relaxation time τ_{fit} as shown in the main manuscript. We also tried to fit our experimental data with the curves we get from our model, but it lead to similar results to the ones obtained using the solution for a homogeneous system. It is worth noting that when we compare the curves in Figure 2a, we observe that in the case of changing D_o the obtained precession curves change in magnitude but not in shape. This means that we do not observe any change in the values obtained for D_{fit} or τ_{fit}. On the other hand, analyzing Figure 2b we see that changes in D_i does not only change the magnitude of the spin signal but also the shape of the curve, which results in changes in D_{fit} with changes in D_i. A similar effect is observed in the analysis of Figure 2c and Figure 2d.

The effect of the sheet resistance on the Hanle precession

The same way as we can change the values for the spin diffusion coefficients and relaxation times for the inner and outer parts (D_o, D_i, τ_o and τ_i) keeping σ_i and σ_i fixed, we can also change the values for the square resistances of the inner and outer regions, $R_i = \sigma_i^{-1}$ and $R_o\sigma_o^{-1}$ respectively. By applying the same procedure of generating a Hanle precession curve and fitting it with the homogeneous model we can extract the effective spin relaxation time τ_{fit} and the effective spin

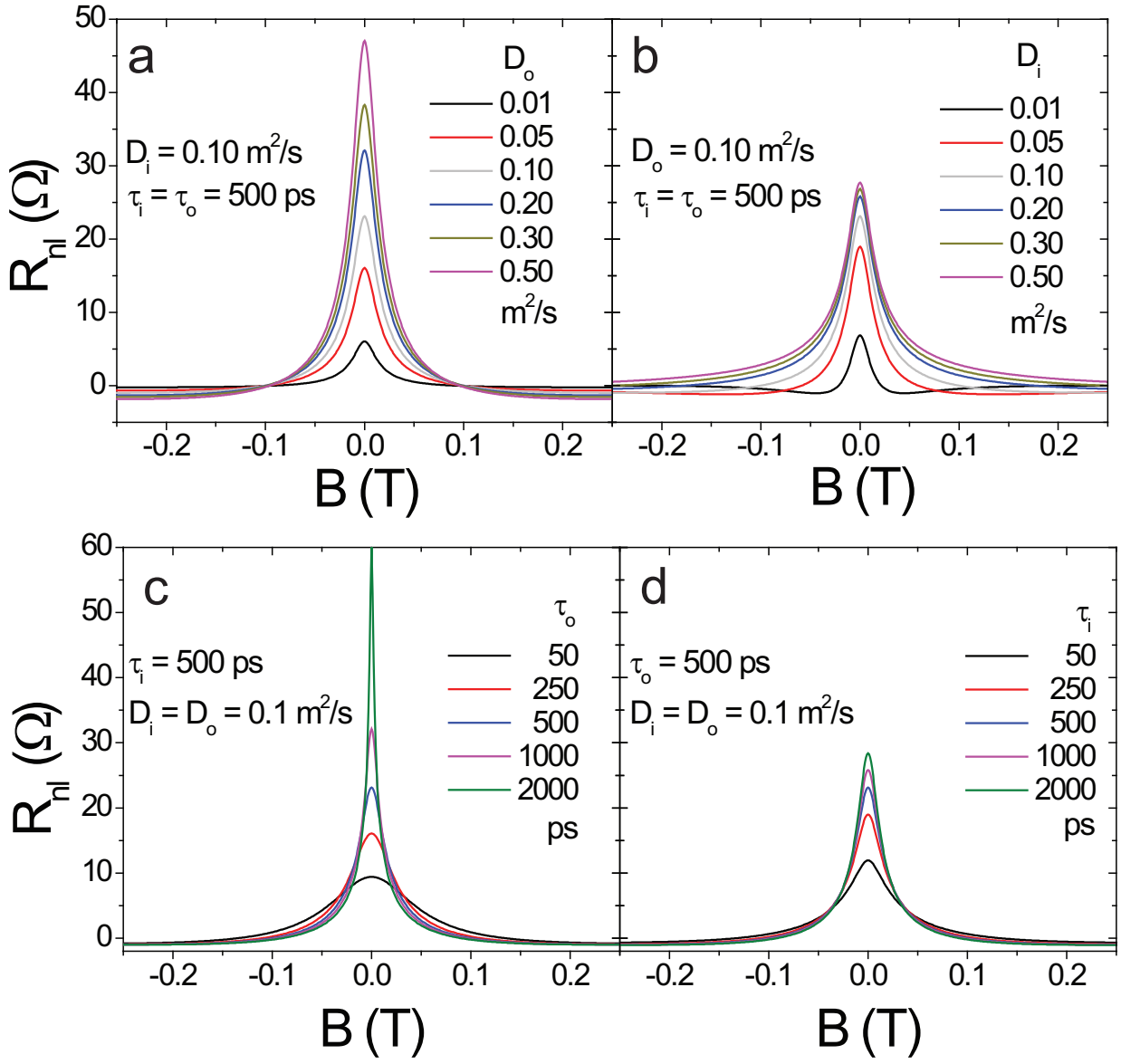

Figure 2: The calculated Hanle precession curves for different values of (a)D_o, (b)D_i, (c)τ_o and (d)τ_i, while keeping the other parameters fixed.

diffusion coefficient D_{fit}. The results for different combinations of R_i and R_o are presented in Figure 3 below.

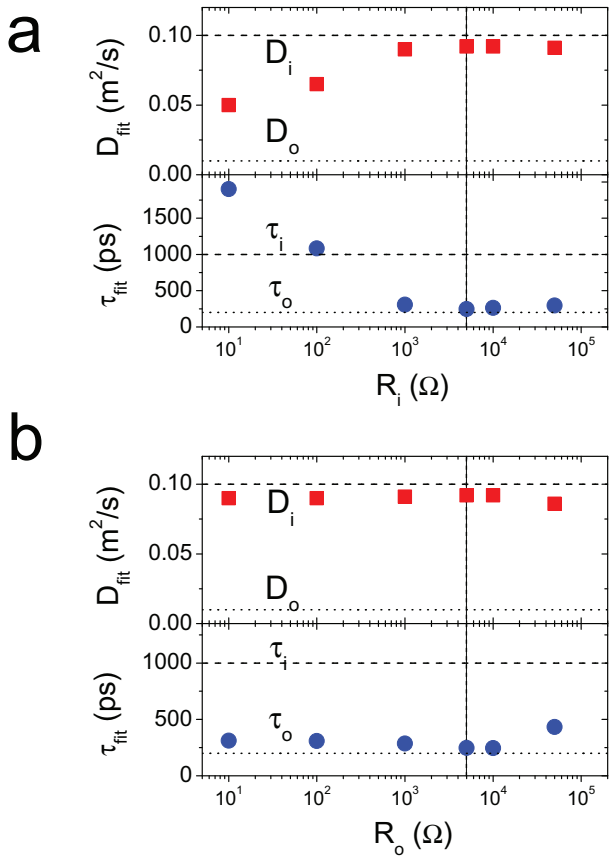

Figure 3: The results obtained for D_{fit} and τ_{fit} for changing (a)R_i and (b)R_o. The outer or inner sheet resistance was kept at 5 kΩ while the other was changed. The values for the diffusion coefficients and spin relaxation times are: D_o=0.01 m^2/s, D_i=0.1 m^2/s, τ_o= 200 ps and τ_i= 1 ns.

As it can be seen in Figure 3 (a) and (b), the conclusions obtained in our main text that D_{fit} is determined mainly by the inner region and τ_{fit} by the outer region remain unchanged when we consider resistances in the range of those we encounter experimentally (1 to 5 kΩ).

References

(1) Tombros, N.; Veligura, A.; Junesch, J.; van den Berg, J. J.; Zomer, P. J.; Wojtaszek, M.; Vera-Marun, I. J.; Jonkman, H. T.; van Wees, B. J. *Journal of Applied Physics* **2011**, *109*, 093702.

(2) Blake, P.; Hill, E. W.; Neto, A. H. C.; Novoselov, K. S.; Jiang, D.; Yang, R.; Booth, T. J.; Geim, A. K. *Applied Physics Letters* **2007**, *91*, 063124.

(3) Abergel, D. S. L.; Russell, A.; Fal'ko, V. I. *Applied Physics Letters* **2007**, *91*, 063125.

(4) Popinciuc, M.; Józsa, C.; Zomer, P. J.; Tombros, N.; Veligura, A.; Jonkman, H. T.; van Wees, B. J. *Phys. Rev. B* **2009**, *80*, 214427.